### Title

Each phospholipase A2 type exhibits distinct selectivity toward sn-1 ester, alkyl ether, and vinyl ether phospholipids




### Journal

Biochimica et Biophysica Acta (BBA) - Molecular and Cell Biology of Lipids, 1867(1)

### ISSN

1388-1981



### Authors

Hayashi, Daiki
Mouchlis, Varnavas D
Dennis, Edward A



### Publication Date

2022

### DOI

10.1016/j.bbalip.2021.159067

Peer reviewed

BBA - Molecular and Cell Biology of Lipids 1867 (2022) 159067

Contents lists available at ScienceDirect

BBA - Molecular and Cell Biology of Lipids

journal homepage: www.elsevier.com/locate/bbalip

# Each phospholipase $A_2$ type exhibits distinct selectivity toward *sn*-1 ester, alkyl ether, and vinyl ether phospholipids

Daiki Hayashi, Varnavas D. Mouchlis, Edward A. Dennis *

*Department of Pharmacology and Department of Chemistry and Biochemistry, University of California, San Diego, La Jolla, CA 92093, USA*

ARTICLE INFO

*Keywords:*
Phospholipase $A_2$
Ether phospholipids
Plasmalogens
Lipidomics
Molecular dynamics simulation

ABSTRACT

Glycerophospholipids are major components of cell membranes and have enormous variation in the composition of fatty acyl chains esterified on the *sn*-1 and *sn*-2 position as well as the polar head groups on the *sn*-3 position of the glycerol backbone. Phospholipase $A_2$ ($PLA_2$) enzymes constitute a superfamily of enzymes which play a critical role in metabolism and signal transduction by hydrolyzing the *sn*-2 acyl chains of glycerophospholipids. In human cell membranes, in addition to the conventional diester phospholipids, a significant amount is the *sn*-1 ether-linked phospholipids which play a critical role in numerous biological activities. However, precisely how $PLA_2$s distinguish the *sn*-1 acyl chain linkage is not understood. In the present study, we expanded the technique of lipidomics to determine the unique *in vitro* specificity of three major human $PLA_2$s, including Group IVA cytosolic $cPLA_2$, Group VIA calcium-independent $iPLA_2$, and Group V secreted $sPLA_2$ toward the linkage at the *sn*-1 position. Interestingly, $cPLA_2$ prefers *sn*-1 vinyl ether phospholipids known as plasmalogens over conventional ester phospholipids and the *sn*-1 alkyl ether phospholipids. $iPLA_2$ showed similar activity toward vinyl ether and ester phospholipids at the *sn*-1 position. Surprisingly, $sPLA_2$ preferred ester phospholipids over alkyl and vinyl ether phospholipids. By taking advantage of molecular dynamics simulations, we found that Trp30 in the $sPLA_2$ active site dominates its specificity for diester phospholipids.

## 1. Introduction

Glycerophospholipids are the defining component of cell membranes, and are composed of two acyl chains esterified to the glycerol backbone at the *sn*-1 and *sn*-2 positions as well as the polar headgroup on the *sn*-3 position. Phospholipase $A_2$ ($PLA_2$) comprises a superfamily of enzymes hydrolyzing the acyl-chain of glycerophospholipids at the *sn*-2 position producing lysophospholipids and free fatty acids [1]. Each $PLA_2$ expresses numerous biological functions, especially in the inflammatory processes, by hydrolyzing membrane glycerophospholipids and producing free fatty acids such as arachidonic acid (20:4, AA) which is an initial substrate of the AA cascade producing bioactive eicosanoids and oxylipins [2]. In addition, importantly $PLA_2$s contribute to membrane remodeling, signal transduction, and "biological surfactants" by producing lysophospholipids which are reacylated with polyunsaturated fatty acids (PUFAs) to produce remodeled phospholipids; lysophospholipids can also be further metabolically converted to ligands for several G-protein coupled receptors (GPCRs); and lysophospholipids as "natural" surfactants/detergents can destabilize membranes exhibiting bacterialcidal effects. These biological functions differ depending on the specific subcellular localization and substrate specificity of each $PLA_2$. Therefore, the substrate specificity and selectivity of each $PLA_2$ is closely correlated with its biological function.

An enormous variety of glycerophospholipids exist based on the combination of acyl chains and head groups and they comprise cell membranes presenting specific morphological and chemical characteristics to the membranes. The enzymatic action of a $PLA_2$ is initiated by its interaction with the lipid-water interface, which is followed by the enzyme extracting a single phospholipid substrate from the membrane to accommodate the specific substrate phospholipid adequately and properly in its active site [3]. Each step contributes to the specific activity of the $PLA_2$, and both the headgroup and the two different acyl chains critically contribute to these steps. For example, Group IVA cytosolic $cPLA_2$ (GIVA $cPLA_2$) shows high activity toward PIP2 containing membranes by interacting specifically with the headgroup at an allosteric site, and Group V secreted $sPLA_2$ (GV $sPLA_2$) preferentially hydrolyzes substrate phospholipids containing phosphatidylglycerol headgroups [4,5]. Also, our previous studies have revealed that the *sn*-2

* Corresponding author.
*E-mail address:* edennis@ucsd.edu (E.A. Dennis).

https://doi.org/10.1016/j.bbalip.2021.159067
Received 22 July 2021; Received in revised form 28 September 2021; Accepted 5 October 2021
Available online 9 October 2021

acyl chain greatly effects substrate specificity [5,6]. In addition, phospholipids contain a variety of linkages at the *sn*-1 position, and this should have some effect on the substrate specificity and selectivity of each $PLA_2$. However, the effect of the *sn*-1 acyl chain on the substrate specificity of each type of $PLA_2$ has not been well understood and this is the focus of this report.

For cellular membranes, *sn*-1 alkyl ether and *sn*-1 vinyl ether-linked phospholipids can account for as much as 20% of the phospholipid, and in addition to the conventional diester glycerophospholipids which have been considered as the primary substrate for $PLA_2$s, the *sn*-1 ether and vinyl ether containing phospholipids can also serve as a substrate for $PLA_2$s. One critical bioactive *sn*-1 alkyl ether phospholipid is 1-*O*-hexadecyl-2-acetyl-*sn*-glycero-3-phosphocholine, which is well known as platelet-activating factor (PAF), and this phospholipid plays a pivotal role in inflammation, platelet activation, and many leucocyte functions [7]. Since lyso-PAF (1-O-alkyl-sn-glycero-3-phosphocholine) is converted to PAF by acylation, $PLA_2$ activity toward the *sn*-1 alkyl ether phospholipids containing AA and other fatty acids at the *sn-2* position as well as toward PAF is important for the synthesis and deactivation of PAF [8]. Indeed, it has been reported that $cPLA_2$ contributes to PAF production [9]. In addition, group VIIA $PLA_2$ (GVIIA $PLA_2$), also known as PAF acetylhydrolase (PAF-AH) as well as being known as lipoprotein-associated $PLA_2$ ($LpPLA_2$), is well recognized as an enzyme responsible for hydrolyzing PAF, and we have demonstrated its substrate specificity and characteristics by taking advantage of lipidomics based techniques and computational approaches [10] (V. Mouchlis et al., manuscript in preparation).

The *sn*-1 vinyl ether phospholipids which are also known as plasmalogens, are the most common *sn*-1 ether-containing phospholipids. Plasmalogens exist ubiquitously but are especially enriched in the brain and heart [11]. It has been suggested that subcellular plasmalogens are abundant in the lipid raft microdomains, where signaling molecules accumulate and contribute to raft formation, although the separation and segmentation of lipid rafts within and from cell membranes are still controversial [12,13]. Further, it has been reported that plasmalogens are involving in membrane trafficking, cell differentiation, and phagocytosis in macrophages and are implicating in various diseases [14–19]. It is known that plasmalogens often contain polyunsaturated fatty acids (PUFAs) in their *sn*-2 acyl chains which are targets for lipid peroxidation. Recently, it has been reported that peroxidation of plasmalogens plays a critical role in cancer ferroptosis [20]. Therefore, regulating ether phospholipids by $PLA_2$ should be critical for many biological responses.

Recently, we have developed lipidomics-based HPLC MS/MS assays using mixed micelles and multiple reaction monitoring (MRM) for various lysophospholipids and demonstrated unique substrate specificity for each of the major groups of human $PLA_2$s including GIVA $cPLA_2$, Group VIA calcium-independent $iPLA_2$ (GVIA $iPLA_2$), and GV $sPLA_2$ focusing on the *sn*-2 acyl chain [5,6]. To date, several studies have reported the *in vitro* activity of $cPLA_2$ toward ether phospholipids [21,22]. However, despite the importance of ether phospholipids in various biological processes, precise *in vitro* specificity and selectivity of $PLA_2$s toward ester and ether phospholipids are still elusive. Herein, we have now applied these lipidomic techniques to *sn*-1 ether phospholipids and report the effect of the ether linkages on the *sn*-1 position to the activity and substrate specificity of the three major types of $PLA_2$. Moreover, by also employing molecular dynamics (MD) simulations, we have now explored the molecular basis of the unique specificity of GV $sPLA_2$ toward ester phospholipids.

## 2. Methods

### 2.1. Materials

All phospholipids, including the lysophospholipid standards employed in this study, were purchased from Avanti Polar Lipids, Inc. The purity of all lipids was greater than 99%. All other materials were of appropriate and suitable quality for this study.

### 2.2. Expression and purification of recombinant human $PLA_2$ enzymes

The human recombinant $PLA_2$s were expressed and purified as described elsewhere [5]. The baculovirus encoding C-terminal 6 × His tag conjugated human GIVA $cPLA_2$, and N-terminal 6 × His tag conjugated human GVIA $iPLA_2$ were used to infect serum free-cultured Sf9 cells with a MOI of 0.1 and 2.0, respectively. The expression was induced for 72 h at 28 °C with shaking. The recombinant protein was purified with Ni-NTA agarose (QIAGEN, Venlo, Netherlands). Elution buffer (25 mM Tris-HCl pH 7.5, 50 mM NaCl, 250 mM imidazole, 30% glycerol, and only for $iPLA_2$, 2 mM ATP was included) was used for elution of recombinant protein. The human GV $sPLA_2$ was expressed using the *E. coli* expression system and refolded by following and modifying the dilution method reported previously [23]. The C-terminal 6 × His tag conjugated human GV $sPLA_2$ was induced for expression with 0.1 mM IPTG for 4 h at 25 °C by using BL21 (DE-3) Gold *E. coli*. The inclusion bodies were collected and denatured in buffer containing 6 M guanidine hydrochloride (GuHCl). Then, the denatured protein was purified with Ni-NTA agarose under the denatured condition. The denatured protein was eluted with elution buffer (25 mM Tris-HCl pH 8.0, 500 mM NaCl, 10 mM β-mercaptoethanol, 250 mM imidazole, 6 M GuHCl), and the eluted solution was dialyzed against dialyzing buffer (50 mM Tris-HCl pH 8.5, 100 mM NaCl, 6 M GuHCl). The protein solution was diluted with refolding buffer (50 mM Tris-HCl pH 8.5, 8.2 mM oxidized glutathione, 9.3 mM reduced glutathione, 12 mM $CaCl_2$ 12% glycerol) at 1: 7 dilution rates added dropwise and incubated for 7 days at 4 °C. Finally, the solution was dialyzed against enzyme buffer (50 mM Tris-HCl pH 8.0, 50 mM NaCl, 10 mM $CaCl_2$, 20% glycerol) to remove GuHCl completely and used as a GV $sPLA_2$ enzyme solution.

### 2.3. Lipidomics-based LC-MS/MS assay

The lipidomics-based LC-MS/MS assay was performed in accord with our previous method [5]. We prepared a substrate mixture containing 100 μM phospholipid, 400 μM C12E8 surfactant, and 2.5 μM 17:0 lysophosphatidylcholine (LPC) as an internal standard. For $cPLA_2$, 3 μM of porcine brain $PIP_2$ (Avanti polar lipids, Inc., Alabaster, AL, USA) was mixed with 97 μM phospholipid to enhance the activity. When we employed mixtures of several different phospholipid substrates, we used a total of 100 μM phospholipid for $iPLA_2$ and $sPLA_2$, or 97 μM phospholipid plus 3 μM $PIP_2$ (as a specific activator) for $cPLA_2$. The reaction was started by adding 5 μl of enzyme solution to 95 μl of substrate solution in a 96-well plate, and the plate was incubated for 30 min at 40 °C with gently shaking. The reaction was quenched by adding 120 μl of methanol/acetonitrile (80/20, *v*/v), and the sample was directly injected into the HPLC-MS/MS system. Mass spectrometry of lysophospholipids was performed with a 4000 QTRAP® (AB Sciex LLC, Framingham MA, USA). The amount of the products was calculated with a standard curve for each product, and the activity was normalized against the protein concentration of the enzyme solution.

### 2.4. Molecular dynamics (MD) simulations

The MD simulations were performed by following our previously published methods [5].

#### 2.4.1. Enzyme-substrate complexes

Initial complexes of GV $sPLA_2$ were generated using our model based on a homology model of GV $sPLA_2$ based on the crystal structure of GIIA $sPLA_2$ [5]. Phospholipids were docked in the active site of each enzyme using the Glide software implemented in the Schrödinger suite using a previously published docking protocol [5,24–26].

#### 2.4.2. Enzyme-membrane systems

The Membrane Builder implemented in CHARMM-GUI was employed to generate enzyme-membrane models for the MD simulations [27,28]. The membrane patch consisted of 1-palmitoyl-2-arachidonoyl-sn-glycero-3-phosphocholine (POPC), 1-stearoyl-2-arachidonoyl-sn-glycero-3-phosphocholine (SAPC), 1-palmitoyl-2-oleoyl-sn-glycero-3-phosphatidic acid (POPA), 1-palmitoyl-2-oleoyl-sn-glycero-3-phosphatidylethanolamine (POPE), 1-palmitoyl-2-oleoyl-sn-glycero-3-phosphatidylglycerol (POPG), 1-palmitoyl-2-oleoyl-sn-glycero-3-phosphatidylserine (POPS), 1-stearoyl-2-arachidonoyl-sn-glycero-3-phosphatidylinositol-4,5-bisphosphate (SAPI(4,5)P2), and cholesterol. The average ratios of the phospholipids were 0.48 for PC, 0.27 for PE, 0.10 for PI(4,5)P2, 0.06 for PS, and 0.09 for PA and PG. The average cholesterol/lipid ratio was 0.40. The composition of the glycerophospholipids (GPL) portion represents the average ratio of the major cellular membranes where the three $PLA_2$s studied are known to be localized and acting. Each system was solvated with TIP3P water molecules and neutralized with 150 mM sodium chloride (NaCl) using the Visual Molecular Dynamics (VMD) package [29].

#### 2.4.3. Equilibration and production runs

Molecular dynamics simulations were carried out using NAMD 2.12 [30]. The minimization and equilibration protocol were performed as follows: a minimization of 80,000 steps was initially performed by applying harmonic constraints on the enzyme-ligand-membrane that were gradually turned off using a constraint scaling factor, followed by a second 120,000 steps minimization without constraints. An initial equilibration of 10,000 steps was performed by also applying harmonic constraints on the enzyme-ligand-membrane that were gradually turned off using the same constraint scaling factor, followed by a second 10,000 steps equilibration without constraints.

Each system was slowly heated and held to 310 K using temperature reassignment with a reassignment frequency of 500 timesteps (1000 fs) and a reassignment increment of 1 K during the equilibration. The minimization and equilibration protocol were sufficient to induce the appropriate disorder of a fluid-like bilayer, avoid unnatural atomistic positions, and failure of the simulations by atoms moving at exceedingly high velocities. Each system was finally subjected to a 1 μs production run. For each production run, the temperature was maintained at 310 K using the Langevin thermostat with Langevin coupling coefficient of 1/ps [31].

The *NPT* ensemble was employed and the pressure was kept constant at 1.01325 kPa using the Langevin piston method with the "useGroupPressure," "useFlexibleCell," and "useConstantArea" parameters turned on [32]. A time step of 2 fs was used in combination with the SHAKE algorithm to hold the bonds of hydrogen atoms similarly constrained [33]. Nonbonded interactions and full electrostatics were calculated every 1 and 2 time steps, respectively. Switching functions were used to smoothly take electrostatic and van der Waals interactions to zero with a switching distance of 10 Å and a cutoff of 12 Å. Long-range electrostatic forces in the periodic system were evaluated using the Particle Mesh Ewald (PME) Sum method with grid spacing 1/Å [34]. The CHARMM General Force Field (CGenFF) and the CHARMM36 all-atom additive force field and parameters were used for the simulations [35,36].

### 2.5. Statistical analysis

All error bars show the standard deviation (SD). A Student's *t*-test was carried out when two groups were compared. A one-way ANOVA followed by the Tukey-Kramer multiple comparison test was carried out when more than three groups were compared using the GraphPad Prism version 5.0. A *p*-value of less than 0.05 was considered to be significant.

## 3. Results

### 3.1. LC-MS/MS assay for ether phospholipids

In contrast to conventional diester phospholipids, *sn*-1 alkyl ether phospholipids and plasmalogens contain alkyl ether and vinyl ether-linked carbon chains on the *sn*-1 position, respectively (Fig. 1A). In this study, *sn*-1 alkyl ether-linked 16:0 and *sn*-1 vinyl ether-linked 18:1 phosphatidylcholine (PC) were used to explore the selectivity of $PLA_2$s toward the *sn*-1 acyl chain linkage. By modifying the MRM setting, we obtained defined peaks for all lyso products, including 17:0 LPC used as an internal standard (Fig. 1B), which resulted in linear standard curves (Fig. 1C).

### 3.2. Specificity of $PLA_2$s toward sn-1 alkyl ether phospholipids

First, we tested the activity of $PLA_2$s toward *sn*-1 alkyl ether PCs and compared the activity with diester PCs which have the same *sn*-2 acyl chains using the LC-MS/MS assay. The *sn*-2 acyl chains were 2:0, 18:1, and 20:4. It is well known that $cPLA_2$ is highly specific toward *sn*-2 20:4 [5] and consistent with that, $cPLA_2$ showed a high specificity toward *sn*-2 20:4 in both diester and alkyl ether phospholipids (Fig. 2A). Also, $cPLA_2$ did not show detectable activity toward *sn*-1 alkyl 16:0, *sn*-2 2:0 PC which is known as PAF, whereas it showed a small activity toward the diester PC 16:0/2:0 (Fig. 2A). The substrate specificity of $iPLA_2$ is more permissive than that of $cPLA_2$ [5] and showed comparable activity toward *sn*-2 18:1 and 20:4 in the *sn*-1 alkyl ether and ester phospholipids (Fig. 2B). However, $iPLA_2$ has minimum activity toward *sn*-2 2:0 in both cases, similar to $cPLA_2$ (Fig. 2B). In contrast, $sPLA_2$ showed better activity toward *sn*-2 2:0 PCs than that of $cPLA_2$ and $iPLA_2$ and high activity toward *sn*-2 18:1 (Fig. 2C). Notably, the *sn*-2 acyl chain specificity of all $PLA_2$s was not affected by the linkage of the *sn*-1 chain. More importantly, all $PLA_2$s showed higher activity toward all diester PCs than that toward alkyl ether PCs (Fig. 2A, B, C).

To eliminate the effect of the shape and characteristics of substrate mixed micelles which might affect the activity of $PLA_2$s, the activity of all three enzymes in equimolar mixtures of diester and *sn*-1 alkyl ether phospholipids was measured. Mixtures of *sn*-2 20:4 phospholipids was used for testing $cPLA_2$, and mixtures of *sn*-2 18:1 phospholipids was used for testing $iPLA_2$ and $sPLA_2$. Even in the mixtures, all $PLA_2$s preferred diester phospholipids (Fig. 2D, E, F). Especially, $sPLA_2$ showed a strong preference toward diester phospholipids, and the activity was more than 4 times higher than that toward *sn*-1 alkyl ether phospholipids (Fig. 2F), whereas $cPLA_2$ and $iPLA_2$ showed 1.6 and 1.7 times higher activity toward diesters than that toward alkyl ethers, respectively (Fig. 2D, E).

### 3.3. Specificity of $PLA_2$s toward sn-1 vinyl ether phospholipids (plasmalogens)

Next, we tested the preference of all three $PLA_2$s for plasmalogens by comparing the activity toward diester phospholipids. In this experiment, PCs which possess 18 carbon chains (C18) on the *sn*-1 position and 18:1, 20:4, and 22:6 on the *sn*-2 position were used. Surprisingly, in contrast to alkyl ether phospholipids, each of the $PLA_2$s tested showed a different preference for plasmalogens. $cPLA_2$ still showed high specificity toward 20:4 in both diester phospholipids and plasmalogens. However, $cPLA_2$ preferred plasmalogens over diester phospholipids (Fig. 3A). $iPLA_2$ showed similar activity in both diester phospholipids and plasmalogens with a similar *sn*-2 acyl chain specificity in both cases (Fig. 3B). $sPLA_2$ showed a high preference for diester phospholipids over plasmalogens (Fig. 3C). Notably, the vinyl ether linkage in plasmalogens did not significantly affect the *sn*-2 acyl chain specificity of all three $PLA_2$s, similar to alkyl ether phospholipids (Fig. 3A, B, C).

Furthermore, even in the mixture of a diester phospholipid and plasmalogen, all three enzymes showed unique preferences. That is, $cPLA_2$ showed double activity toward plasmalogens comparing to

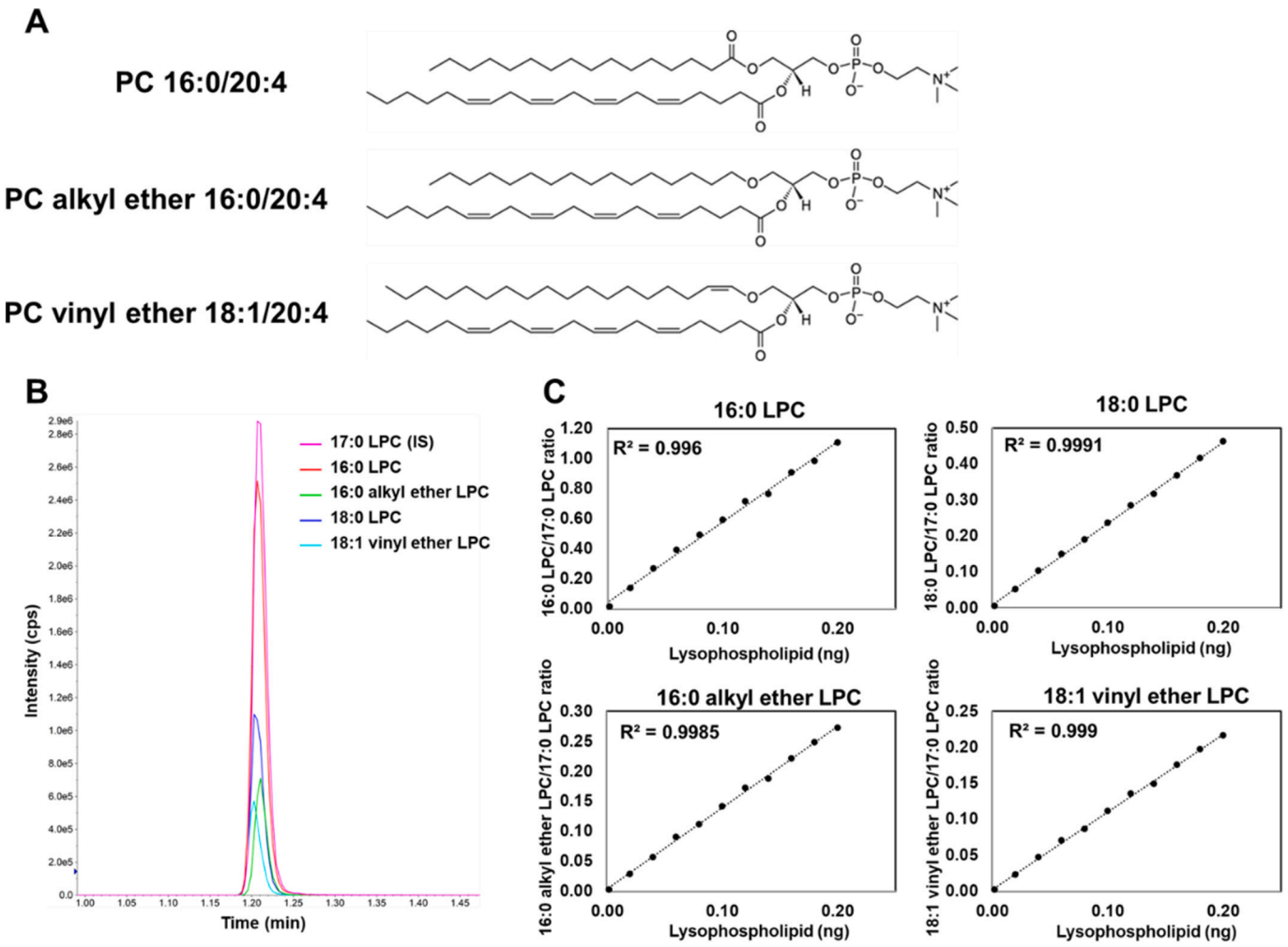


**Fig. 1.** LC-MS/MS analysis of *sn*-1 ester, alkyl ether, and vinyl ether. (A) Structures for diester *sn*-1 16:0, *sn*-2 20:4 PC (PC 16:0/20:4), *sn*-1 alkyl ether 16:0, *sn*-2 20:4 PC (PC alkyl ether 16:0/20:4), and *sn*-1 vinyl ether, 18:1 *sn*-2 20:4 (PC vinyl ether 18:1/20:4). (B) Chromatogram of lyso-PC (LPC) products. 17:0 LPC was used as an internal standard (IS). (C) Standard curves for 16:0 LPC, 18:0 LPC, 16:0 alkyl ether LPC, and 18:1 vinyl ether LPC used for quantification of $PLA_2$ activity.

diester phospholipids (Fig. 3D), while $iPLA_2$ does not have any strong preference between plasmalogen and diester phospholipid (Fig. 3E). Of special note is the fact that $sPLA_2$ showed a strong preference for diester phospholipids, namely, 7.5 times higher $sPLA_2$ activity toward diester phospholipids than plasmalogens was detected (Fig. 3F).

### 3.4. *Specificity of $PLA_2$s in complex mixtures of all substrates*

Finally, to confirm a preference for the linkage of the *sn*-1 acyl chain, we tested complex mixtures of the *sn*-1 alkyl ether, plasmalogen, and ester phospholipids. We mixed *sn*-1 16:0 alkyl ether and ester and separately *sn*-1 C18 vinyl ether and ester phospholipids equally and used them as a substrates in the LC-MS/MS assay. The *sn*-2 acyl chain of 20:4 was selected for $cPLA_2$, and 18:1 was selected for $iPLA_2$ and $sPLA_2$. Consistent with previous results, $cPLA_2$ showed the highest activity toward plasmalogens over diester and alkyl ether phospholipids and some preference toward diester phospholipids over alkyl ether phospholipids (Fig. 4A). $iPLA_2$ also showed a small preference toward diester phospholipids comparing to alkyl ether phospholipids, but there was no significant difference in the activity toward plasmalogen and diester phospholipids (Fig. 4B). $sPLA_2$ exhibited a significantly higher preference for diester phospholipids comparing to alkyl ethers and plasmalogens by approximately 3.2 and 5.6-fold, respectively (Fig. 4C). From these results, it became clear that the three major types of human $PLA_2$s each exhibit a unique *in vitro* preference for the linkage of the *sn*-1 acyl chain in addition to the *sn*-2 acyl chain. In other words, these results suggest that $PLA_2$s recognize the *sn*-1 acyl chain linkage in addition to the *sn*-2 acyl chain and this directly affects substrate specificity.

### 3.5. *Binding mode of ether and ester phospholipids in the $sPLA_2$ active site*

To explore the molecular basis by which $PLA_2$ senses the *sn*-1 acyl chain linkage, we performed 1 μsec MD simulations which analyzed the binding of the *sn*-1 alkyl ether or ester 16:0, *sn*-2 18:1 PC in the $sPLA_2$ active site since $sPLA_2$ showed more dramatic selectivity toward the *sn*-1 linkage than the other $PLA_2$s. We started with the optimal binding mode of the optimal substrate in the $sPLA_2$ active site. After a 1 μsec simulation, although the binding pose of the *sn*-2 acyl chain was slightly different, both the ether and the ester substrates placed their *sn*-2 carbonyl groups, which are attacked upon the hydrolysis reaction, near the catalytic histidine (His47) (Fig. 5A, and B). The *sn*-2 acyl chain of the ester PC penetrated the hydrophobic subsite constituted by Leu5, Ile9, Tyr21, Val95, and Leu98 by stretching the chain and appeared stable in the hydrophobic pocket compared to the binding pose of the ether PC (Fig. 5A and B). Indeed, the binding free energy of the ester PC calculated by the MM-GBSA method was lower than that of the ether PC (ester: −67.01 and ether: −64.12). For the head group binding, Arg62 mainly contributes to the binding by its hydrogen bonds with high occupancy (ester: 51.85% and ether: 56.96%) in both cases (Fig. 5A and B, and Movie 1 and 2). In addition to Arg62, Gly31 takes part in the binding

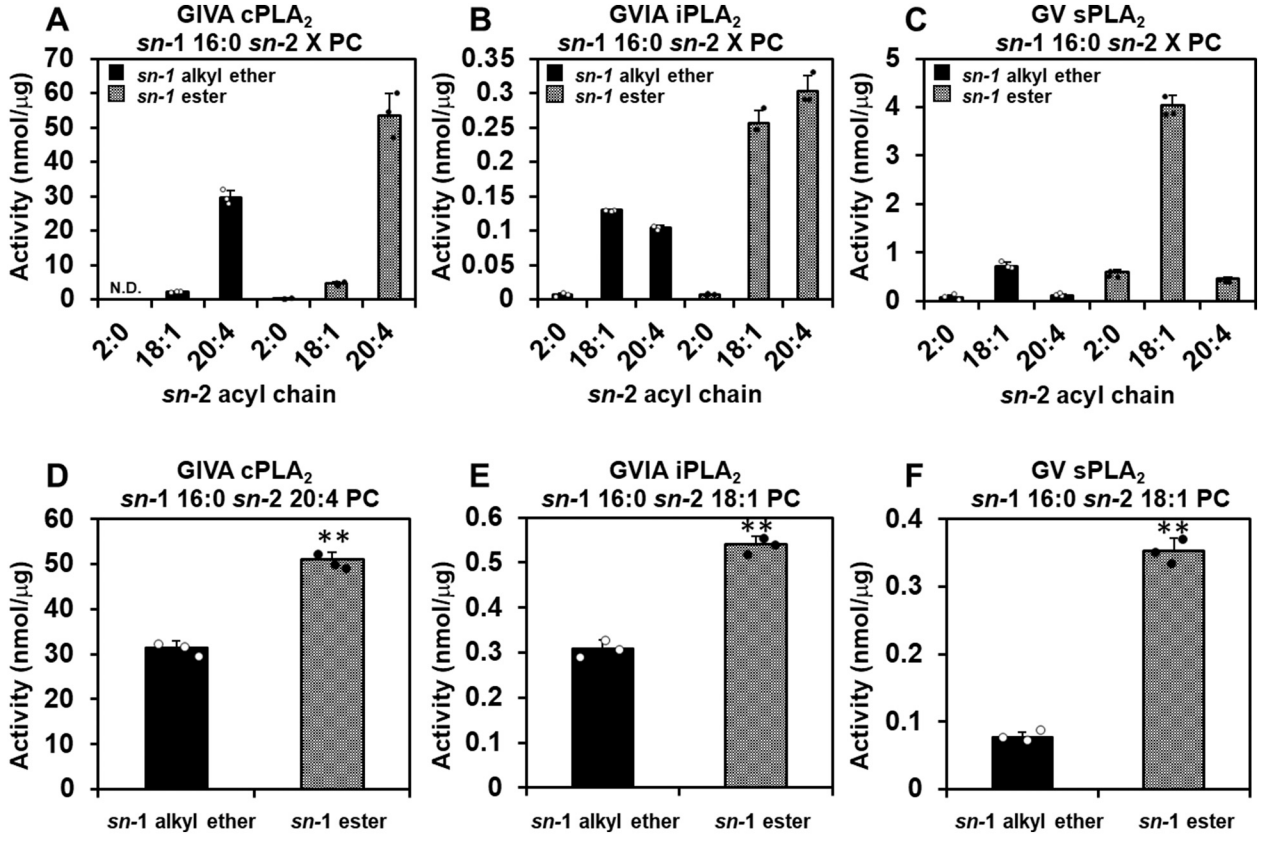


**Fig. 2.** Enzyme activity of $PLA_2$s toward *sn*-1 alkyl ether phospholipids and diester phospholipids. The activity of (A) GIVA $cPLA_2$, (B) GVIA $iPLA_2$, and (C) GV $sPLA_2$ is shown toward *sn*-1 alkyl ether or ester 16:0 *sn*-2 X PC, where X is 2:0, 18:1, or 20:4. (D) The activity of GIVA $cPLA_2$ toward *sn*-1 alkyl ether or ester 16:0 *sn*-2 20:4 PC in equal proportions with 100 μM total phospholipid. The activity of (E) GVIA $iPLA_2$ and (F) GV $sPLA_2$ toward *sn*-1 alkyl ether or ester 16:0 *sn*-2 18:1 PC in equal proportions with 100 μM total phospholipid. The amount of lyso products were determined and quantified using authentic LPC primary and internal standards. Error bars show standard deviation (SD). N.D.: not detected. Asterisks indicate statistical significance. $^{**}P < 0.01$.

of the head group of the ether PC (Fig. 5B and Movie 2). Interestingly, it turned out that Trp30 formed a hydrogen bond with the *sn*-1 carbonyl oxygen in the case of the ester PC (Fig. 5A), while due to lack of the oxygen, the interaction with Trp30 was not part of the binding of the ether PC (Fig. 5B). In the simulation of the ester PC, Trp30 seemed to help the precise binding of the substrate in the active site by interacting with the *sn*-1 carbonyl group at the early steps of the simulation (Movie 1). However, ether PC does not possess the oxygen, and alternative interactions between Trp30 and the ether oxygen appear to trap the substrate away from the catalytic histidine at the early steps of the simulation (Movie 2). Indeed, the distance between the catalytic histidine to the *sn*-2 carbonyl group of the ester PC reached its optimal distance by 300 ns, but the ether PC took 700 ns to reach the optimal distance (Fig. 5C). In other words, thanks to the interaction between the *sn*-1 carbonyl group and Trp30, ester phospholipids are more rapidly precisely accommodated comparing to ether phospholipids. This appears to contribute to the high preference of $sPLA_2$ toward ester phospholipids.

## 4. Discussion

We have previously explored the substrate specificity of $PLA_2$s and their molecular basis, especially focusing on the variety of head groups and *sn*-2 acyl chains [5]. Several decades ago, the activity of $cPLA_2$ toward plasmalogens and alkyl ether phospholipids was reported [21,22], and a plasmalogen-selective $PLA_2$ was characterized [37]. However, the precise *in vitro* selectivity of major human groups of $PLA_2$ toward the precise linkage of the *sn*-1 acyl chain has been elusive. The present study reveals the unique *in vitro* preference of three important human $PLA_2$s for the ether as well as the vinyl ether linkage of the *sn*-1 acyl chain by expanding on our previously developed lipidomics-based LC-MS/MS assay. Moreover, by taking advantage of MD simulations, we can now rationalize the molecular basis of GV $sPLA_2$s unique recognition of the *sn*-1 acyl chain linkage.

### 4.1. $cPLA_2$ activity toward plasmalogens

Interestingly, the current studies revealed that the *in vitro* activity of GIVA $cPLA_2$ toward plasmalogens is higher than that toward conventional ester phospholipids. GIVA $cPLA_2$ is highly specific for *sn*-2 AA and plays a critical role in the production of pro-inflammatory eicosanoids by providing free AA [2,5]. Typically, polyunsaturated fatty acids, especially AA, occupy the *sn*-2 acyl chain of plasmalogens [38]. Therefore, plasmalogens can be a major source of AA hydrolyzed by GIVA $cPLA_2$. Also, it has been reported that $cPLA_2$ deficient mice exhibit impaired brain DHA metabolism, implicating $cPLA_2$ in the metabolism of DHA in the brain [39]. It is well recognized that the *in vitro* activity of $cPLA_2$ toward *sn*-2 DHA is remarkably low, and our previous study agreed with and documented this conclusion [5]. Therefore, how $cPLA_2$ could contribute to the metabolism of DHA in the brain was enigmatic. The current study revealed that the activity of $cPLA_2$ toward plasmalogen DHA was approximately 4.5-fold higher than that of the diester (Fig. 3A). Interestingly, this ratio was much higher than the ratio between plasmalogen AA and diester AA (approximately 1.7-fold). In addition, it is well known that the brain is enriched with both plasmalogens and DHA [11,40].

In the current study, we utilized PC plasmalogens to maintain a constant head group for the three different *sn*-1 linkages. However, it is

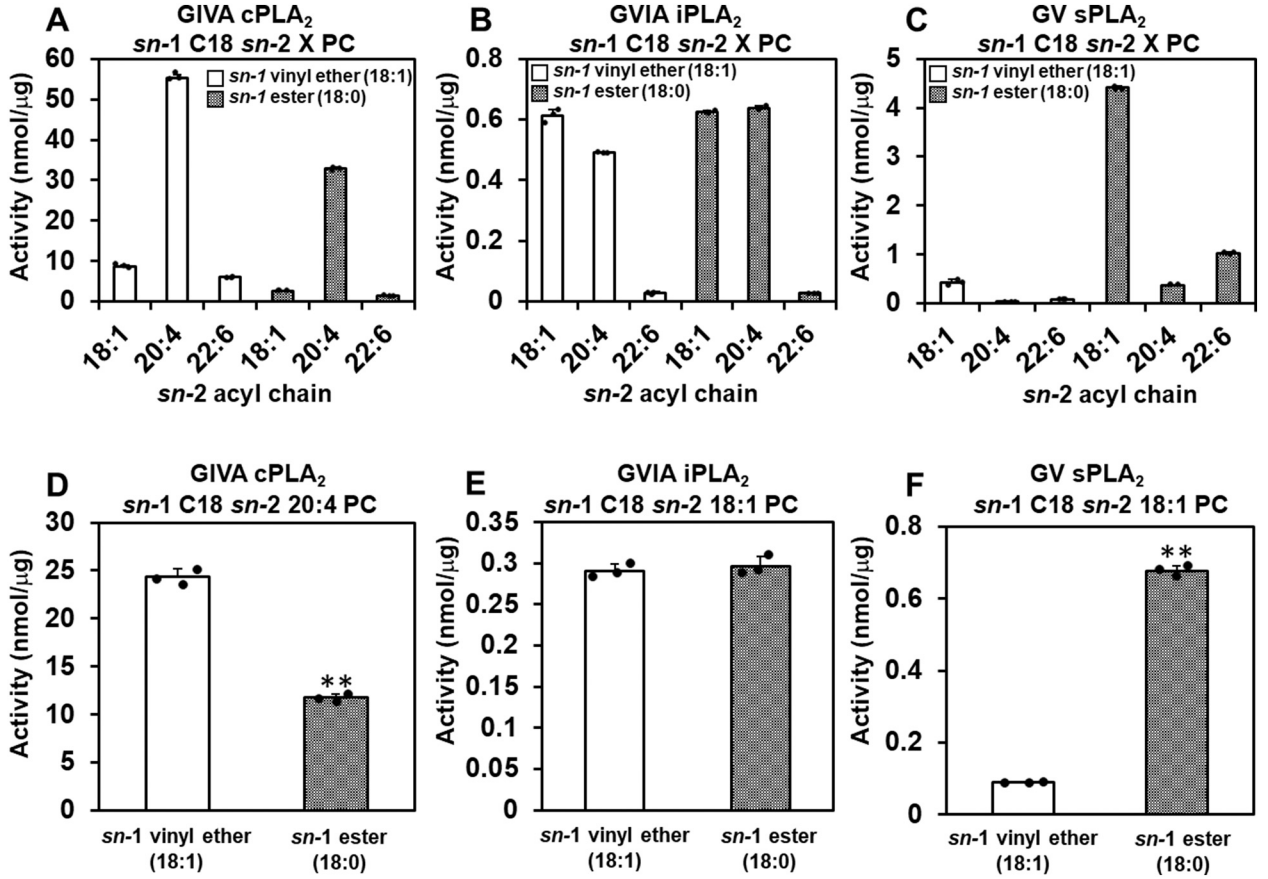


**Fig. 3.** Enzyme activity of $PLA_2$s toward *sn*-1 vinyl ether phospholipids and diester phospholipids. The activity of (A) GIVA $cPLA_2$, (B) GVIA $iPLA_2$, and (C) GV $sPLA_2$ is shown toward *sn*-1 vinyl ether or ester C18 *sn*-2 X PC, where X is 18:1, 20:4, or 22:6. (D) The activity of GIVA $cPLA_2$ toward *sn*-1 vinyl ether or ester C18 *sn*-2 20:4 PC in equal proportions with 100 μM total phospholipid. The activity of (E) GVIA $iPLA_2$ and (F) GV $sPLA_2$ toward *sn*-1 vinyl ether or ester C18 *sn*-2 18:1 PC in equal proportions with 100 μM total phospholipid. The amount of lyso products were determined and quantified using authentic LPC primary and internal standards. Error bars show SD. Asterisks indicate statistical significance. $^{**}P < 0.01$.

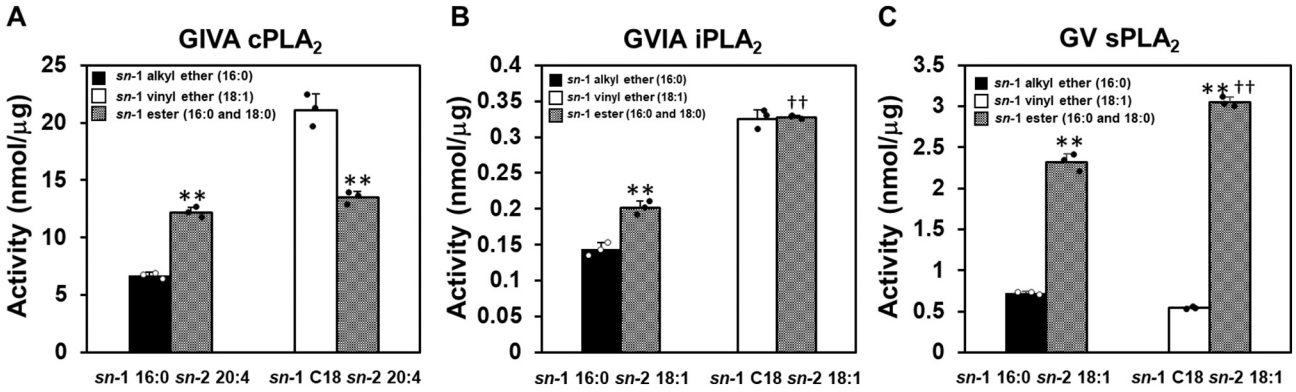


**Fig. 4.** Enzyme activity of $PLA_2$s in complex mixtures of phospholipids. (A) The activity of GIVA $cPLA_2$ toward *sn*-1 alkyl ether or ester 16:0, *sn*-2 20:4 (16:0/20:4) and *sn*-1 vinyl ether or ester C18, *sn*-2 20:4 (18:0 or 18:1/20:4) PC in equal proportions with 100 μM total phospholipid. The activity of (B) GVIA $iPLA_2$ and (C) GV $sPLA_2$ toward *sn*-1 alkyl ether or ester 16:0, *sn*-2 18:1 (16:0/18:1) and *sn*-1 vinyl ether or ester C18, *sn*-2 18:1 (18:0 or 18:1/18:1) PC in equal proportions with 100 μM total phospholipid. The amount of lyso products were determined and quantified using authentic LPC primary and internal standards. Error bars show SD. Asterisks indicate statistical significance. $^{**}P < 0.01$ (comparison between the substrate which has the same number of carbons on the *sn*-1 position), $^{††}P < 0.01$ (comparison between the ester phospholipids).

well known that phosphatidylethanolamine (PE) is the dominant head group for plasmalogens in the human brain. Our previous study indicated that the head group did not significantly affect the specificity of $cPLA_2$ in a mixture of phospholipids [5]. Therefore, a similar effect for the *sn*-1 linkage for $cPLA_2$ activity would be expected in PE plasmalogens. Accordingly, $cPLA_2$ is more likely to hydrolyze DHA esterified plasmalogens, rather than diester phospholipids containing DHA, thereby contributing to DHA metabolism in the brain.

### 4.2. *In vitro* vs *in vivo* activity of phospholipase $A_2$s

The *in vitro* preference of $PLA_2$s is not always translatable directly to

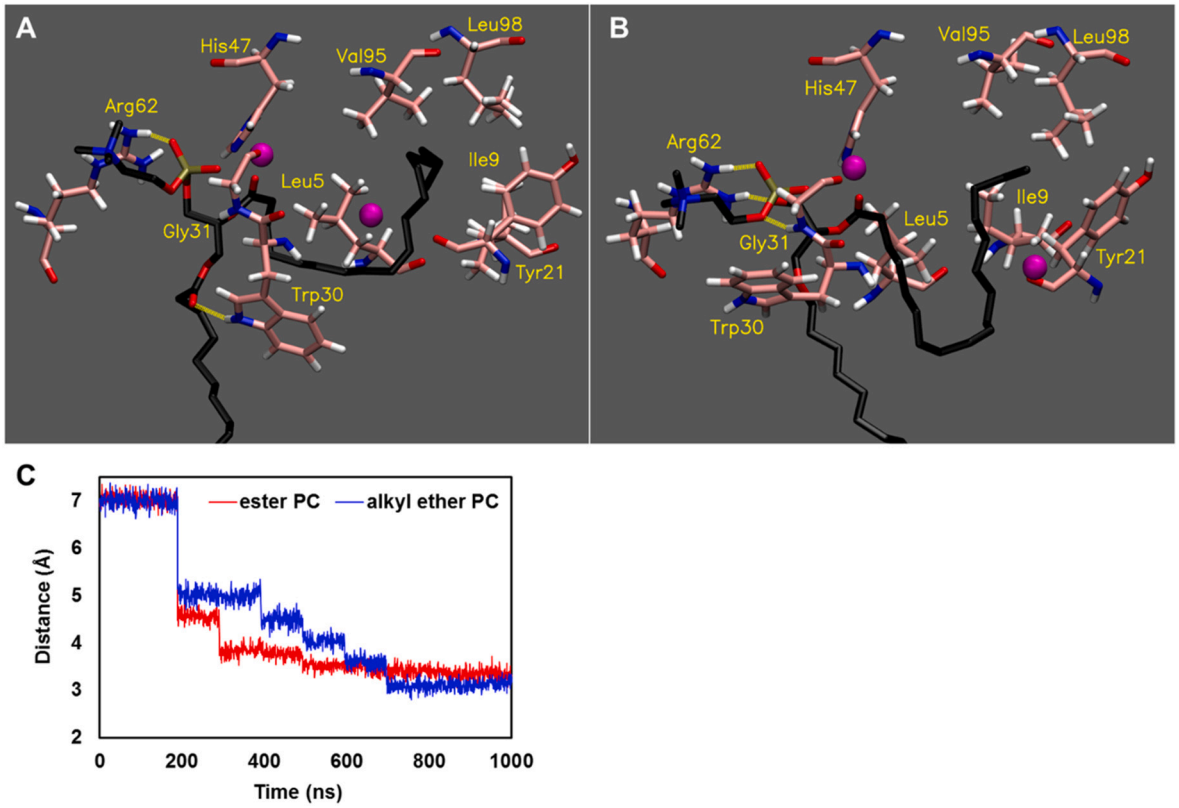


**Fig. 5.** Binding of ester and alkyl ether PC in the active site of $sPLA_2$. The image of the final frame of the 1 μsec simulations for (A) *sn*-1 ester 16:0, *sn*-2 18:1 PC and (B) *sn*-1 alkyl ether 16:0, *sn*-2 18:1 PC is shown in the optimal binding mode. Movie 1 and Movie 2 show the result of the entire 1 μs simulation for *sn*-1 ester 16:0, *sn*-2 18:1 PC and *sn*-1 alkyl ether 16:0, *sn*-2 18:1 PC, respectively. The purple spheres represent $Ca^{2+}$, and the yellow dashed lines represent hydrogen bonds (distance cutoff: 3.2 Å, angle cutoff: 30°). (C) The distance from His47 to the carbonyl group of each *sn*-2 acyl chain over the 1 μsec simulations is shown.

the *in vivo* situation. Indeed, a study using a murine macrophage cell line reports that the AA mobilization, which is due to $cPLA_2$, is independent of the plasmalogen content [41]. It has also been reported that $cPLA_2$ contributes to lyso-PAF production, although $cPLA_2$ showed the lowest activity toward *sn*-1 alkyl ether phospholipids [9]. Also, our data indicates that $iPLA_2$ slightly, but significantly, prefers the *sn*-1 palmitoyl ester phospholipid over the *sn*-1 stearoyl ester (Fig. 4B). However, GVIA $iPLA_2$ reportedly utilizes the *sn*-1 palmitoylated substrate upon zymosan stimulation of mouse macrophages [42], and $iPLA_2$-overexpressed HEK293 cells [43]. These facts indicate that the preference of each $PLA_2$ *in vivo* can be limited by the availability of the specific phospholipid pool, specific stimulus, and subcellular localization of both substrates and enzyme, although the *in vitro* preference can show a different underlying preference or selectivity for them to hydrolyze a certain substrate. Indeed, it has been reported that $iPLA_2$ utilizes plasmalogens for AA release in a murine macrophage cell line. However, in plasmalogen-deficient murine macrophage cells, $iPLA_2$ utilizes ester phospholipids without any effect on the amount of released AA, which is consistent with *in vitro* specificity of $iPLA_2$ [44].

In the current study, we took advantage of detergent/phospholipid mixed micelles as substrate because the vesicle-based assay does not work well for detailed kinetic comparisons (for example, due to lag phases, linearity of the enzyme activity toward varying GPLs is often not seen and phospholipid vesicles of pure phospholipids vary in curvature, and can't be formed for certain phospholipids). Since the mixed micelles are mainly composed of nonionic surfactant/detergent molecules, the surface where $PLA_2$s interact is an artificial environment, although natural biological membranes are very heterogeneous collections of molecules including proteins and carbohydrates and combinations thereof. However, as described above, the *in vivo* specificity of $PLA_2$s are limited by many factors including enzyme as well as optimal substrate abundance and localization at the site of enzyme action.

Our *in vitro* assay reveals the inate catalytic ability of each enzyme toward a certain substrate. Therefore, it is expected that a difference would be observed between the *in vitro* specificity of each $PLA_2$ toward each specific phospholipid substrate in mixed micelles and specifically formulated phospholipid vesicles, as well as when using natural isolated biological membranes as substrates. Differences would be expected to be especially notable when comparing *in vitro* specificity results under very controlled and exacting conditions as reported herein with physiological observations in cells and tissues.

### 4.3. $sPLA_2$ preference for diester substrates

Among the three human $PLA_2$s, GV $sPLA_2$ showed remarkable preference toward diester phospholipids. $sPLA_2$ is a 14 kDa small enzyme and has 7 disulfide bonds which make the structure rigid. Due to these characteristics, $sPLA_2$ only accommodates the *sn*-2 acyl chain and head group in its active site, whereas $cPLA_2$ and $iPLA_2$ accommodate phospholipid substrates entirely [5]. In other words, the tail of the *sn*-1 acyl chain of phospholipids that are bound to $sPLA_2$ remains in the lipid bilayer and the lipid-water interface. The MD simulation showed that Trp30 critically contributes to the binding pose of substrates by interacting with the carbonyl group of the *sn*-1 acyl chain and confers a unique preference for the ester phospholipids. However, in addition to this interaction, there is the possibility that the differing chemical properties of ester, ether, and vinyl ethers affects the substrate preference of $sPLA_2$.

Specifically, the carbonyl oxygen on the *sn*-1 acyl chain can contribute to the stabilization of the *sn*-1 acyl chain in the lipid-water interface, and this characteristic might help explain the remarkable preference of the GV $sPLA_2$ toward diester phospholipids over ether and

vinyl ether phospholipids. Upon the binding of GV $sPLA_2$ to the lipid membrane, Trp30 is localized at the water-membrane interface. It was reported that substitution of the Trp30 of GV $sPLA_2$ by Ala significantly suppressed interfacial binding to the zwitterionic phospholipid surface and its activity [45]. Therefore, it appears that Trp30 is contributing to interfacial binding as well as the *sn*-1 linkage selectivity and is critical for the function of GV $sPLA_2$. For the MD simulations, we utilized the ester and alkyl ether PC for comparison of the binding assuming that the reason that the addition of the vinylic double bond does not lead to a significant additional activity effect is that $sPLA_2$ fails to recognize the *sn*-1 double bond.

In this study with substrate-docked GV $sPLA_2$, we have shown the importance of the *sn*-1 acyl chain linkage in the binding pose of the substrates in the active site. However, it is also important to note that the *sn*-1 acyl chain linkage contributes to the extraction of substrate. $PLA_2$ extracts a single phospholipid from the cell membrane and stabilizes the orientation of the substrate so as to hydrolyze the substrate. Therefore, each step appears to contribute to the substrate specificity of $PLA_2$s, although further experimental data and modeling studies are needed. Indeed, for example, Lys725 of $iPLA_2$ is suggested to be critical for extracting the substrate into its active site [3]. In the current studies, we performed 1 μsec simulations to show the binding of substrates, and the time seemed to be long enough since the distance from the *sn*-2 carbonyl group to the catalytic histidine reached and settled at a reasonable distance expected for catalytic function by the end of the simulations. However, the time scale for enzymatic cleavage of the substrate is still elusive and beyond the scope of these computational methods. Of course, the question of whether accommodation of the substrate in its optimal binding mode is the rate-limiting step needs further clarification.

## 5. Conclusion

In the present study, we revealed the *in vitro* selectivity of the three major types of human $PLA_2$ toward the linkage of the *sn*-1 acyl chain, and this selectivity can be related to their biological function. Moreover, we detailed the molecular basis of the selectivity of GV $sPLA_2$, which shows a dramatic preference toward ester phospholipids over alkyl ethers and vinyl ethers according to MD simulations and suggest that similar types of effects could influence the detailed molecular basis of the selectivity of GIVA $cPLA_2$ and GVIA $iPLA_2$ toward the *sn*-1 linkage, though they are less extreme. However, this study raised the importance of analyzing ether and vinyl ether containing phospholipids as well as diester phospholipids as substrates for $PLA_2$s in all biological studies if one wants to understand and explore the entire role of $PLA_2$s *in vivo*.

Supplementary data to this article can be found online at https://doi.org/10.1016/j.bbalip.2021.159067.

## CRediT authorship contribution statement

D. H. performed the experiments and analyzed the data. V. D. M. performed the MD simulations. D. H., V. D. M., and E. A. D. wrote the manuscript. E. A. D. supervised the research.

## Declaration of competing interest

The authors declare that they have no known competing financial interests or personal relationships that could have appeared to influence the work reported in this paper.

## Acknowledgments

This work was supported by NIH grants RO1 GM20501-45 and R35 GM139641-01 (E.A.D.) and a postdoctoral fellowship from The Uehara Memorial Foundation in Japan (D.H.). We sincerely thank Prof. Oswald Quehenberger and Aaron Armando for their support with the LC-MS/MS system in our laboratory.

## References

[1] E.A. Dennis, J. Cao, Y.H. Hsu, V. Magrioti, G. Kokotos, Phospholipase A2 enzymes: physical structure, biological function, disease implication, chemical inhibition, and therapeutic intervention, Chem. Rev. 111 (2011) 6130–6185, https://doi.org/10.1021/cr200085w.
[2] E.A. Dennis, P.C. Norris, Eicosanoid storm in infection and inflammation, Nat. Rev. Immunol. 15 (2015) 511–523, https://doi.org/10.1038/nri3859.
[3] V.D. Mouchlis, D. Bucher, J.A. McCammon, E.A. Dennis, Membranes serve as allosteric activators of phospholipase a2, enabling it to extract, bind, and hydrolyze phospholipid substrates, Proc, Natl. Acad. Sci. U. S. A. 112 (2015) E516–E525, https://doi.org/10.1073/pnas.1424651112.
[4] S. Das, W. Cho, Roles of catalytic domain residues in interfacial binding and activation of group IV cytosolic phospholipase A2, J. Biol. Chem. 277 (2002) 23838–23846, https://doi.org/10.1074/jbc.M202322200.
[5] V.D. Mouchlis, Y. Chen, J. Andrew McCammon, E.A. Dennis, Membrane Allostery and unique hydrophobic sites promote enzyme substrate specificity, J. Am. Chem. Soc. 140 (2018) 3285–3291, https://doi.org/10.1021/jacs.7b12045.
[6] D. Hayashi, V.D. Mouchlis, E.A. Dennis, Omega-3 versus Omega-6 fatty acid availability is controlled by hydrophobic site geometries of phospholipase A2s, J. Lipid Res. (2021), 100113, https://doi.org/10.1016/j.jlr.2021.100113.
[7] S.M. Prescott, G.A. Zimmerman, D.M. Stafforini, T.M. McIntyre, Platelet-activating factor and related lipid mediators, Annu, Rev. Biochem. 69 (2000) 419–445, https://doi.org/10.1146/annurev.biochem.69.1.419.
[8] R.L. Wykle, B. Malone, F. Snyder, Enzymatic synthesis of 1-alkyl-2-acetyl-sn-glycero-3-phosphocholine, a hypotensive and platelet-aggregating lipid, J. Biol. Chem. 255 (1980) 10256–10260.
[9] S.A. Bauldry, R.E. Wooten, Leukotriene B4 and platelet activating factor production in permeabilized human neutrophils: role of cytosolic PLA2 in LTB4 and PAF generation, Biochim. Biophys. Acta 1303 (1996) 63–73.
[10] L.W. Tjoelker, C. Eberhardt, J. Unger, Hai Le Trong, G.A. Zimmerman, T.M. McIntyre, D.M. Stafforini, S.M. Prescott, P.W. Gray, Plasma platelet-activating factor acetylhydrolase is a secreted phospholipase A2 with a catalytic triad, J. Biol. Chem. 270 (1995) 25481–25487. doi:https://doi.org/10.1074/jbc.270.43.25481.
[11] N.E. Braverman, A.B. Moser, Functions of plasmalogen lipids in health and disease, Biochim. Biophys. Acta - Mol. Basis Dis. 1822 (2012) 1442–1452. doi:https://doi.org/10.1016/j.bbadis.2012.05.008.
[12] L.J. Pike, X. Han, K.N. Chung, R.W. Gross, Lipid rafts are enriched in arachidonic acid and plasmenylethanolamine and their composition is independent of caveolin-1 expression: a quantitative electrospray ionization/mass spectrometric analysis, Biochemistry. 41 (2002) 2075–2088, https://doi.org/10.1021/bi0156557.
[13] C. Rodemer, T.P. Thai, B. Brugger, T. Kaercher, H. Werner, K.A. Nave, F. Wieland, K. Gorgas, W.W. Just, Inactivation of ether lipid biosynthesis causes male infertility, defects in eye development and optic nerve hypoplasia in mice, Hum. Mol. Genet. 12 (2003) 1881–1895, https://doi.org/10.1093/hmg/ddg191.
[14] D. Komljenovic, R. Sandhoff, A. Teigler, H. Heid, W.W. Just, K. Gorgas, Disruption of blood-testis barrier dynamics in ether-lipid-deficient mice, Cell Tissue Res. 337 (2009) 281–299, https://doi.org/10.1007/s00441-009-0809-7.
[15] A. Teigler, D. Komljenovic, A. Draguhn, K. Gorgas, W.W. Just, Defects in myelination, paranode organization and Purkinje cell innervation in the ether lipid-deficient mouse cerebellum, Hum. Mol. Genet. 18 (2009) 1897–1908, https://doi.org/10.1093/hmg/ddp110.
[16] T. Tsukahara, R. Tsukahara, S. Yasuda, N. Makarova, W.J. Valentine, P. Allison, H. Yuan, D.L. Baker, Z. Li, R. Bittman, A. Parrill, G. Tigyi, Different residues mediate recognition of 1-O-oleyl-lysophosphatidic acid and rosiglitazone in the ligand binding domain of peroxisome proliferator-activated receptor, J. Biol. Chem. 281 (2006) 3398–3407, https://doi.org/10.1074/jbc.M510843200.
[17] M.S. Hossain, K. Mineno, T. Katafuchi, Neuronal orphan G-protein coupled receptor proteins mediate plasmalogens-induced activation of ERK and Akt signaling, PLoS One 11 (2016) 1–14, https://doi.org/10.1371/journal.pone.0150846.
[18] J.M. Dean, I.J. Lodhi, Structural and functional roles of ether lipids, Protein Cell. 9 (2018) 196–206, https://doi.org/10.1007/s13238-017-0423-5.
[19] J.M. Rubio, A.M. Astudillo, J. Casas, M.A. Balboa, J. Balsinde, Regulation of phagocytosis in macrophages by membrane ethanolamine plasmalogens, Front. Immunol. 9 (2018) 1–14, https://doi.org/10.3389/fimmu.2018.01723.
[20] Y. Zou, W.S. Henry, E.L. Ricq, E.T. Graham, V.V. Phadnis, P. Maretich, S. Paradkar, N. Boehnke, A.A. Deik, F. Reinhardt, J.K. Eaton, B. Ferguson, W. Wang, J. Fairman, H.R. Keys, V. Dančík, C.B. Clish, P.A. Clemons, P.T. Hammond, L.A. Boyer, R. A. Weinberg, S.L. Schreiber, Plasticity of ether lipids promotes ferroptosis susceptibility and evasion, Nature. 585 (2020) 603–608, https://doi.org/10.1038/s41586-020-2732-8.
[21] E. Diez, P. Louis-Flamberg, R.H. Hall, R.J. Mayer, Substrate specificities and properties of human phospholipases A2 in a mixed vesicle model, J. Biol. Chem. 267 (1992) 18342–18348.
[22] A.M. Hanel, S. Schüttel, M.H. Gelb, Processive interfacial catalysis by mammalian 85-kilodalton phospholipase A2 enzymes on product-containing vesicles: application to the determination of substrate preferences, Biochemistry. 32 (1993) 5949–5958, https://doi.org/10.1021/bi00074a005.
[23] F. Giordanetto, D. Pettersen, I. Starke, P. Nordberg, M. Dahlström, L. Knerr, N. Selmi, B. Rosengren, L.O. Larsson, J. Sandmark, M. Castaldo, N. Dekker, U. Karlsson, E. Hurt-Camejo, Discovery of AZD2716: a novel secreted phospholipase A2 (sPLA2) inhibitor for the treatment of coronary artery disease,

ACS Med, Chem. Lett. 7 (2016) 884–889, https://doi.org/10.1021/acsmedchemlett.6b00188.
[24] V.D. Mouchlis, D. Limnios, M.G. Kokotou, E. Barbayianni, G. Kokotos, J. A. McCammon, E.A. Dennis, Development of potent and selective inhibitors for group VIA calcium-independent phospholipase A2 guided by molecular dynamics and structure-activity relationships, J. Med. Chem. 59 (2016) 4403–4414, https://doi.org/10.1021/acs.jmedchem.6b00377.
[25] R.A. Friesner, R.B. Murphy, M.P. Repasky, L.L. Frye, J.R. Greenwood, T.A. Halgren, P.C. Sanschagrin, D.T. Mainz, Extra precision glide: docking and scoring incorporating a model of hydrophobic enclosure for protein-ligand complexes, J. Med. Chem. 49 (2006) 6177–6196, https://doi.org/10.1021/jm051256o.
[26] V.D. Mouchlis, C. Morisseau, B.D. Hammock, S. Li, J.A. McCammon, E.A. Dennis, Computer-aided drug design guided by hydrogen/deuterium exchange mass spectrometry: a powerful combination for the development of potent and selective inhibitors of Group VIA calcium-independent phospholipase A2, Bioorganic Med, Chem. 24 (2016) 4801–4811, https://doi.org/10.1016/j.bmc.2016.05.009.
[27] E.L. Wu, X. Cheng, S. Jo, H. Rui, K.C. Song, E.M. Dávila-Contreras, Y. Qi, J. Lee, V. Monje-Galvan, R.M. Venable, J.B. Klauda, W. Im, CHARMM-GUI membrane builder toward realistic biological membrane simulations, J. Comput. Chem. 35 (2014) 1997–2004, https://doi.org/10.1002/jcc.23702.
[28] J. Lee, X. Cheng, J.M. Swails, M.S. Yeom, P.K. Eastman, J.A. Lemkul, S. Wei, J. Buckner, J.C. Jeong, Y. Qi, S. Jo, V.S. Pande, D.A. Case, C.L. Brooks, A. D. MacKerell, J.B. Klauda, W. Im, CHARMM-GUI input generator for NAMD, GROMACS, AMBER, OpenMM, and CHARMM/OpenMM simulations using the CHARMM36 additive force field, J. Chem. Theory Comput. 12 (2016) 405–413, https://doi.org/10.1021/acs.jctc.5b00935.
[29] W. Humphrey, A. Dalke, K. Schulten, VMD: visual molecular dynamics, J. Mol. Graph. 14 (1996) 33–38, https://doi.org/10.1016/0263-7855(96)00018-5.
[30] J.C. Phillips, R. Braun, W. Wang, J. Gumbart, E. Tajkhorshid, E. Villa, C. Chipot, R. D. Skeel, L. Kalé, K. Schulten, Scalable molecular dynamics with NAMD, J. Comput. Chem. 26 (2005) 1781–1802, https://doi.org/10.1002/jcc.20289.
[31] S.A. Adelman, J.D. Doll, Generalized Langevin equation approach for atom/solid-surface scattering: general formulation for classical scattering off harmonic solids, J. Chem. Phys. 64 (1976) 2375–2388, https://doi.org/10.1063/1.432526.
[32] S.E. Feller, Y. Zhang, R.W. Pastor, B.R. Brooks, Constant pressure molecular dynamics simulation: the Langevin piston method, J. Chem. Phys. 103 (1995) 4613–4621, https://doi.org/10.1063/1.470648.
[33] J.P. Ryckaert, G. Ciccotti, H.J.C. Berendsen, Numerical integration of the cartesian equations of motion of a system with constraints: molecular dynamics of n-alkanes, J. Comput. Phys. 23 (1977) 327–341, https://doi.org/10.1016/0021-9991(77)90098-5.
[34] U. Essmann, L. Perera, M.L. Berkowitz, T. Darden, H. Lee, L.G. Pedersen, A smooth particle mesh Ewald method, J. Chem. Phys. 103 (1995) 8577–8593, https://doi.org/10.1063/1.470117.
[35] K. Vanommeslaeghe, E. Hatcher, C. Acharya, S. Kundu, S. Zhong, J. Shim, E. Darian, O. Guvench, P. Lopes, I. Vorobyov, A.D. Mackerell, CHARMM general force field: a force field for drug-like molecules compatible with the CHARMM all-atom additive biological force fields, J. Comput. Chem. 31 (2010) 671–690, https://doi.org/10.1002/jcc.21367.
[36] J.B. Klauda, R.M. Venable, J.A. Freites, J.W. O'Connor, D.J. Tobias, C. Mondragon-Ramirez, I. Vorobyov, A.D. MacKerell, R.W. Pastor, Update of the CHARMM all-atom additive force field for lipids: validation on six lipid types, J. Phys. Chem. B 114 (2010) 7830–7843, https://doi.org/10.1021/jp101759q.
[37] J. McHowat, S. Liu, M.H. Creer, Selective hydrolysis of plasmalogen phospholipids by Ca2 -independent PLA2 in hypoxic ventricular myocytes, Am. J. Phys. 274 (1998) 1727–1737.
[38] R.W. Gross, High plasmalogen and arachidonic acid content of canine myocardial sarcolemma: a fast atom bombardment mass spectroscopic and gas chromatography-mass spectroscopic characterization, Biochemistry (1984), https://doi.org/10.1021/bi00296a026.
[39] T.A. Rosenberger, N.E. Villacreses, M.A. Contreras, J.V. Bonventre, S.I. Rapoport, Brain lipid metabolism in the cPLA2 knockout mouse, J. Lipid Res. 44 (2003) 109–117, https://doi.org/10.1194/jlr.M200298-JLR200.
[40] N. Salem, B. Litman, H.Y. Kim, K. Gawrisch, Mechanisms of action of docosahexaenoic acid in the nervous system, Lipids. 36 (2001) 945–959, https://doi.org/10.1007/s11745-001-0805-6.
[41] P. Lebrero, A.M. Astudillo, J.M. Rubio, L. Fernández-Caballero, G. Kokotos, M. A. Balboa, J. Balsinde, Cellular Plasmalogen content does not influence arachidonic acid levels or distribution in macrophages: a role for cytosolic phospholipase A2γ in phospholipid remodeling, Cells. 8 (2019), https://doi.org/10.3390/cells8080799.
[42] L. Gil-de-Gómez, A.M. Astudillo, C. Guijas, V. Magrioti, G. Kokotos, M.A. Balboa, J. Balsinde, Cytosolic group IVA and calcium-independent group VIA phospholipase a 2 s act on distinct phospholipid pools in zymosan-stimulated mouse peritoneal macrophages, J. Immunol. 192 (2014) 752–762, https://doi.org/10.4049/jimmunol.1302267.
[43] M. Murakami, S. Masuda, K. Ueda-Semmyo, E. Yoda, H. Kuwata, Y. Takanezawa, J. Aoki, H. Arai, H. Sumimoto, Y. Ishikawa, T. Ishii, Y. Nakatani, I. Kudo, Group VIB Ca2+−independent phospholipase A2γ promotes cellular membrane hydrolysis and prostaglandin production in a manner distinct from other intracellular phospholipases A2, J. Biol. Chem. 280 (2005) 14028–14041, https://doi.org/10.1074/jbc.M413766200.
[44] D.P. Gaposchkin, H.W. Farber, R.A. Zoeller, On the importance of plasmalogen status in stimulated arachidonic acid release in the macrophage cell line RAW 264.7, Biochim. Biophys. Acta - Mol. Cell Biol. Lipids. 1781 (2008) 213–219. doi: https://doi.org/10.1016/j.bbalip.2008.01.007.
[45] S.K. Han, K.P. Kim, R. Koduri, L. Bittova, N.M. Munoz, A.R. Leff, D.C. Wilton, M. H. Gelb, W. Cho, Roles of Trp31 in high membrane binding and proinflammatory activity of human group V phospholipase A2, J. Biol. Chem. 274 (1999) 11881–11888, https://doi.org/10.1074/jbc.274.17.11881.